Concepts for Experiments at Future Colliders I

PD Dr. Oliver Kortner

11.11.2024

Hadron showers

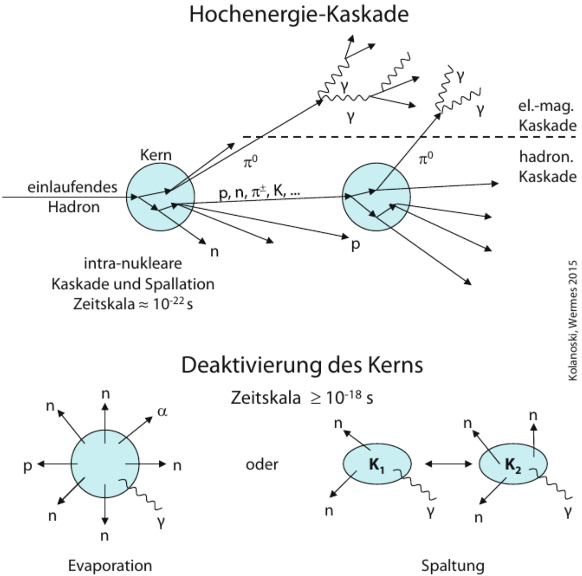

Similar behaviour like electromagnetic showers:

- Shower length proportional to $\lambda_A \approx 35\ \text{g cm}^{-2} \frac{A^{1/3}}{\rho} \gg X_0$.
- Transverse size independent of the energy of the primary hadron: λ_A.
- But much stronger variations of the shower size than in case of electromagnetic showers.

Recapitulation of the previous lecture

Shower components and shower fluctuations

Contributions to the energy E_{dep} deposited in a block of material

$$E_{dep} = (\underbrace{f_{em} + \underbrace{f_{ion} + f_n + f_\gamma + f_B}_{=:f_h}}_{=1 \text{ per definitionem}})E_{dep}$$

- f_{em}. Fraction of the energy deposited by photons from π^0 decays. As neutral pions are created again and again, f_{em} increases with the particle multiplicity in the cascade, hence with the energy of the incoming hadron.
- f_{ion}. Fraction of the energy deposited by a charged shower particle by ionization.
- f_n. Fraction of the energy deposited by neutrons via elastic scattering or nuclear reactions.
- f_γ. Fraction of the energy deposited by photons which are created in nuclear reactions. $E_\gamma \sim$ keV...MeV $\Rightarrow$ energy transfer by Compton scattering or photoelectric effect. This contribution can occur with a large delay $\gtrsim \mu$s.
- f_B. The binding energy which is required to break up a nucleus is not measured and does not contribute to the calorimeter signal. One has a similar situation with neutrinos which are usually take into account in f_B.

Recapitulation of the previous lecture

Shower components and shower fluctuations

Contribution of the energy E_{dep} deposited to a block of matter

$$E_{dep} = \underbrace{(f_{em} + \underbrace{f_{ion} + f_n + f_\gamma + f_B}_{=:f_h})}_{=1 \text{ per definitionem}} E_{dep}$$

- f_{em} varies strongly in a hadronic shower between 0 and 1 if no or only neutral pions are generated in the first interactions.
- The composition of the hadron component is independent of the type and energy of the incoming hadron.

Concepts for future colliders

Recapitulation of the previous lecture

Future cicular colliders as an origins explorer

Experiments at future circular colliders will allow us to address the following questions:

Origin of matter

Electroweak phase transition, CP violation, baryogenesis, ecc.

Origins of the Higgs boson

Sypersymmetry, compositeness, ecc.

Origins of flavour

Beyond the Standard Model flavour models.

Origin of dark matter

So-called "dark sector" in general.

Origin of neutrinos

Beyond Standard Model neutrino modesl, neutrino portal, ecc.

Origin of the Standard Model

The Standard Model is ultimately an effective field theory of an underlying UV theory from which it originates.

For further information see "The physics case for next-generation colliders" by Tevong You (https://indico.cern.ch/event/1273702/timetable/?view=standard)

Recapitulation of the previous lecture

Current roadmap

Approved projects

- LHC operation until mid 2026.
- HL-LHC operation from 2030 to $\sim$2040.

Future projects (to be approved)

- e^+e^- linear or circular collider.
- 100 TeV hadron collider.

Likely future: A circular e^+e^- collider in a ring of 91.1 km circumference at CERN around 2042 followed by a 100 TeV proton proton collider in the same ring around 2060, i.e. first FCC-ee, than FCC-hh.

Concepts for future colliders

Goals:
- Precision tests of the Standard Model.
- Search for new particles or interactions.

Method: Study of collisions of highly energetic particles.

- The colliding particles must be electrically charged so that they can be accelerated.
- The colliding particles must be stable so that they can be accumulated in a storage ring.

⇒ Only two particles can be used:
  - Electrons (and positrons)
  - protons (and antiprotons)

Basic principle of a collider

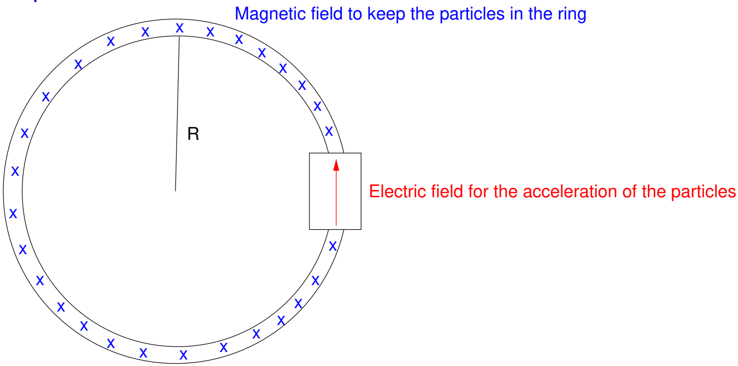

- The size of the magnetic field B and the radius of the ring R determine the maximum achievable beam energy.

$$p = eBR$$

- LHC: B=8 T, R=4,3 km, d.h. $p \approx$10 TeV.
- FCC: B=16 T, $R \approx$16 km, d.h. $p \approx$70 TeV.

Luminosity and event rate

(Instantaneous) luminosity

$$\mathcal{L} = \frac{n_b f_r n_1 n_2}{A}$$

- n_b: Number of particle bunches in the storage ring.
- f_r: Collision frequency.
- $n_{1,2}$: Number of the protons in the colliding bunches.
- A: Effective area of the colliding particle bunches.

Event rate

$$\sigma_{pp \to X} \cdot \mathcal{L}$$

e^+e^- collider vs pp collider

Particle	Advantages	Disadvantages
$e^\pm$	$e^\pm$ elementary particles	Creation of a lot of synchrotron radiation in circular colliders
p ($\bar{p}$)	Less synchrotron radiation due to higher mass acceleration to very high energies in circular colliders	Proton composite particle. Collision of partons.

- The only option for collisions at centre-of-mass energies $\gtrsim$10 TeV: pp collisions.
- $p\bar{p}$ not advantageous, because
  - parton luminosities of pp and $p\bar{p}$ are similar and
  - much lower luminosities are achievable for $p\bar{p}$ than for pp, because it is difficult to generate and accumulate sufficiently many antiprotons.

High-energy e^+e^- accelerator landscape

Mogens Dam

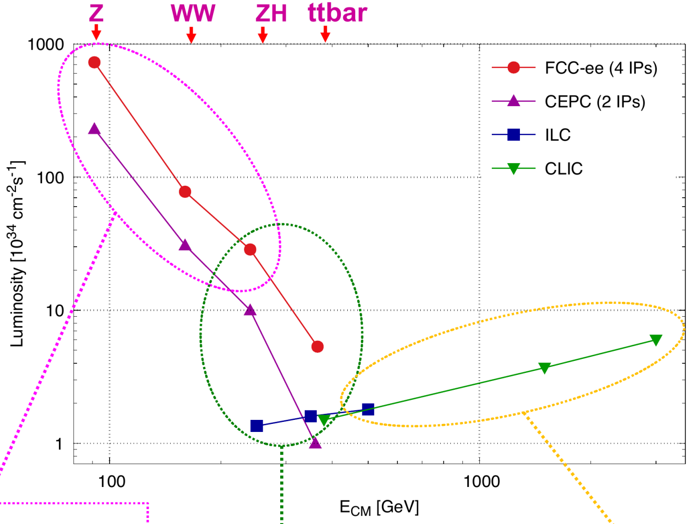

Circular colliders
Extremely high luminosities at lower energies:
Z, W, Higgs, and top factories

Overlap region, 240-380 GeV
Higgs Factories (and top)

Linear colliders
High centre-of-mass energies

Recapitulation of the previous lecture

FCC-ee physics landscape

Mogens Dam

"Higgs Factory" Programme

- At two energies, 240 and 365 GeV, collect in total
  - 2M HZ events and 125k WW → H events
- Higgs couplings to fermions and bosons
- Higgs self-coupling (2-4 σ) via loop diagrams
- Unique possibility: measure electron coupling in s-channel production $e^+e^- \rightarrow H$ @ $\sqrt{s}$ = 125 GeV

Ultra Precise EW Programme & QCD

Measurement of EW parameters with factor ~300 improvement in *statistical* precision wrt current WA

- 6×10^{12} hadronic Z and 2×10^{8} WW
  - m_Z, Γ_Z, Γ_{inv}, $\sin^2\theta_W^{eff}$, R^Z_ℓ, R_b, α_s, m_W, Γ_W...
- 2×10^{6} tt
  - m_{top}, Γ_{top}, EW couplings

Indirect sensitivity to new phys. up to Λ=70 TeV scale

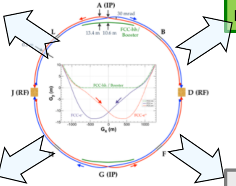

Heavy Flavour Programme

- Enormous statistics: 1.3×10^{12} bb, cc; 2.8×10^{11} ττ
- Extremely clean environment, favourable kinematic conditions (boost) from Z decays
- CKM matrix, CP measurements, "flavour anomaly" studies, e.g. b → sττ, rare decays, CLFV searches, lepton universality, PNMS matrix unitarity

Feebly Coupled Particles - LLPs

Intensity frontier: Opportunity to directly observe new feebly interacting particles with masses below m_Z:

- Axion-like particles, dark photons, Heavy Neutral Leptons
- Signatures: long lifetimes – LLPs

Let us move to hadron (pp) colliders!

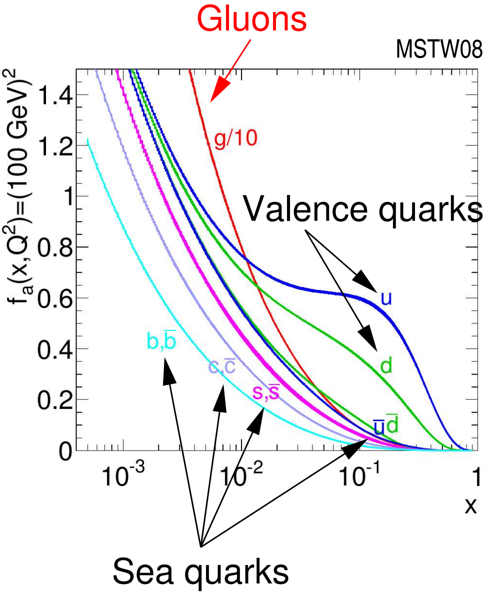

x: Fraction of the proton momentum carried by a single parton.

Q: Momentum scale of the parton collision.

$$\sqrt{s_{Parton\ 1, Parton\ 2}} = \sqrt{x_1 \cdot x_2}\sqrt{s_{pp}},$$

i.e. collisions with $\sqrt{s_{Parton\ 1, Parton\ 2}} = \sqrt{s_{pp}}$ are very rare.

Parton luminosity

General formula for the cross section of a process:

$$\sigma_{pp\to X} = \sum_{a,b=q,g} \int_0^1 \int_0^1 \hat{\sigma}_{ab\to X} \cdot \underbrace{f_a(x_a, Q^2) \cdot f_b(x_b, Q^2)}_{\text{partonluminosity}} dx_a dx_b$$

$\hat{\sigma}_{ab\to X}$: Cross section of the process at parton level.

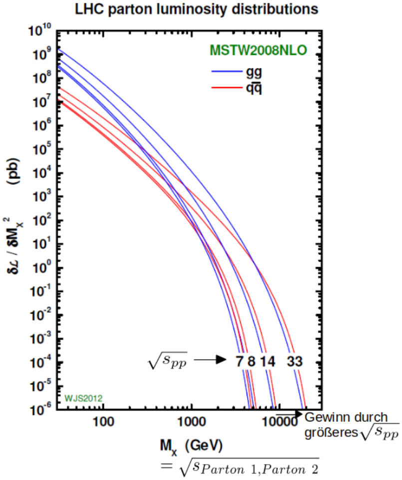

- Parton luminosities increase with $\sqrt{s_{pp}}$ because more and more sea quarks and gluons will be created.
- Gluons dominate at small values of $\sqrt{s_{parton\ 1, parton\ 2}}$ because the parton densities are dominated by gluons at small values of x.

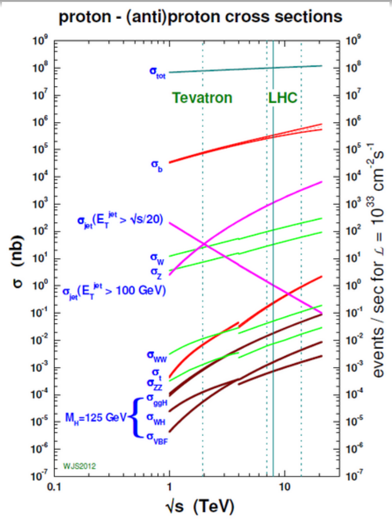

- σ increases with $\sqrt{s_{pp}}$.
- σ for interesting processes like the production of Higgs bosons very small and much smaller than for QCD processes as $pp \to b\bar{b}$.

$\Rightarrow$
- Large pp collision rates (large luminosity) required to become sensitive to rare processes.
- Selective triggers for the selection of interesting pp collisions mandatory.

Hadron collider strategy for the next years

- Increase the LHC luminosity by an order of magnitude $\to$ HL-LHC.
- Increase the centre-of-mass energy $\sqrt{s_{pp}}$ by an order of magnitude $\to$ FCC-hh.

Future hadron colliders

Future hadron colliders

- HL-LHC: $\sqrt{s} = 14$ TeV, $\int \mathcal{L} dt = 3$ ab^{-1}
  Increase of the LHC's luminosity by an order of magnitude with improved beam optics in the collision zones.
- FCC-hh: $\sqrt{s} = 100$ TeV, $\int \mathcal{L} dt = 30$ ab^{-1}
  Increase of the center-of-mass energy with a new storage ring of the four time the circumference of the LHC ring and dipole magnets with twice the field strength.

Most importants goals of the physics programmes (without details)

- HL-LHC
  - Measurement of the properties of the Higgs boson, in particular observation of the decay $H \to \mu^+\mu^-$ and of first evidence of Higgs boson pair production.
  - Search for physics beyond the Standard Model.
- FCC-hh
  - Precision measurements of Higgs boson properties, especially the study of the Higgs boson pair production for the exploration of the structure of the Higgs boson self-coupling.
  - Search for physics beyond the Standard Model.

FCC-CDR

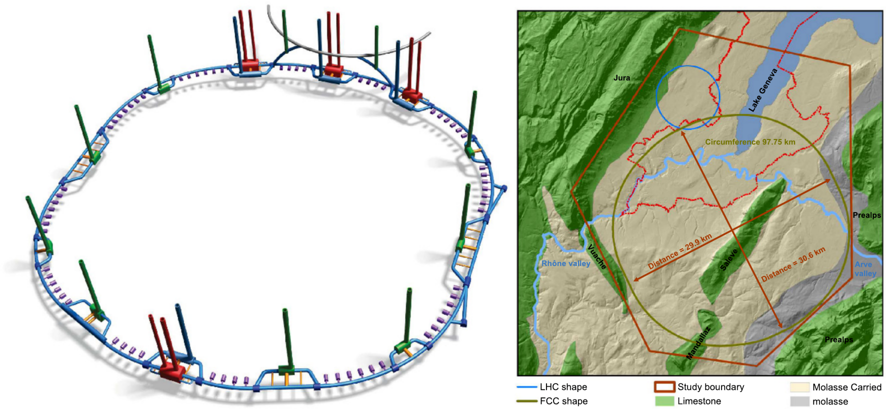

Fig. 2. Left: 3D, not-to-scale schematic of the underground structures. Right: study boundary (red polygon), showing the main topographical and geological structures, LHC (blue line) and FCC tunnel trace (olive green line).

Dipole magnets for the FCC-hh

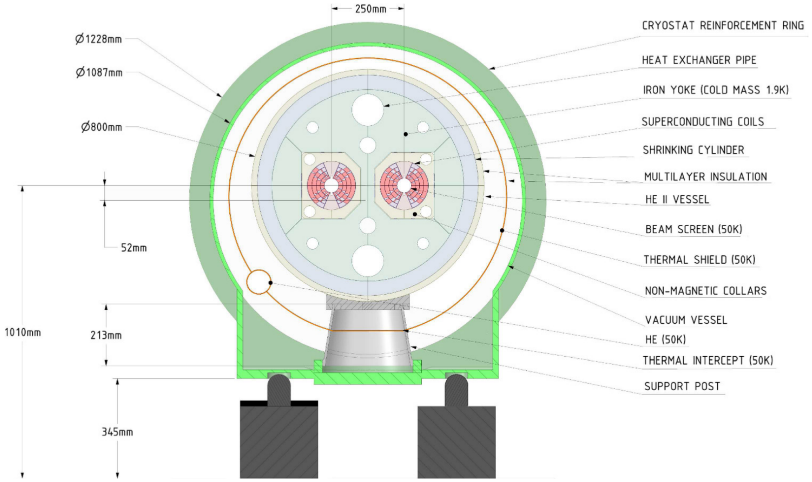

Fig. 3.1. Main dipole cross-section.

- Plan to use Nb_3Sn wires as superconductors in magents.

⇒ Achievable field strength: 16 T $\Rightarrow \sqrt{s} = 100$ TeV.

Comparison of the HL-LHC and the FCC-hh

	LHC	HL-LHC	FCC-hh Initial	FCC-hh Nominal
Physics performance and beam parameters				
Peak luminosity[1] (10^{34} cm^{-2}s^{-1})	1.0	5.0	5.0	<30.0
Optimum average integrated luminosity/day (fb^{-1})	0.47	2.8	2.2	8
Peak number of inelastic events/crossing	27	135 levelled	171	1026
Total/inelastic cross section σ proton (mbarn)	111/85		153/108	
Beam parameters				
Number of bunches n	2808		10 400	
Bunch spacing (ns)	25	25	25	
Bunch population N (10^{11})	1.15	2.2	1.0	

- Similar operating conditions at the FCC-hh in the initial phase like at the HL-LHC.

⇒ Detectors which will were developed for the HL-LHC are suitable for the operation at the FCC-hh in phase 1.

- Evolution of the HL-LHC detectors for the areas of very high particle fluxes needed.

Example of a collision event at the HL-LHC

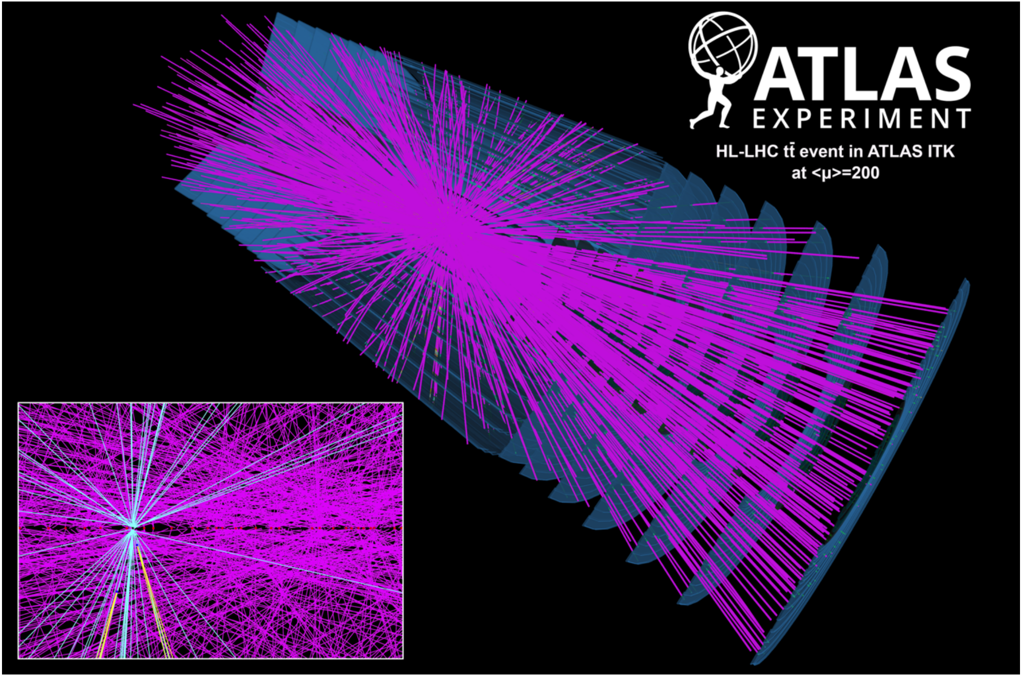

Basic structure of a particle detector at a hadron collider

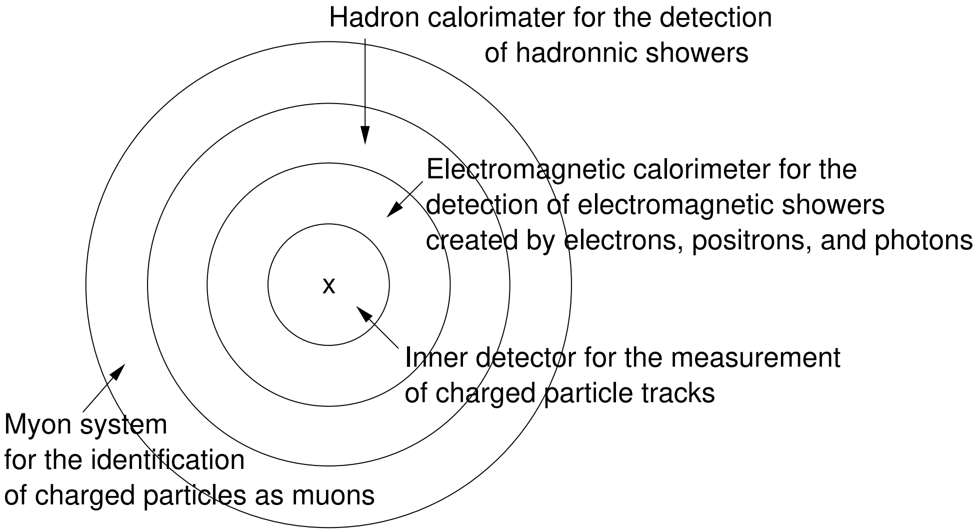

- As explained in the previous lecture, cross sections are much smaller in e^+e^- collission than in pp collisions because only electroweak processes are accessible in the e^+e^- vertex while there is a huge total pp because the partons also interact strongly.

$\Rightarrow$ Much smaller particle fluxes and particle multiplicities in the detectors at an e^+e^- than at a pp collider.

$\Rightarrow$ Different requirements for the detectors.

e^+e^- collision event

Higgs event in e⁺e⁻

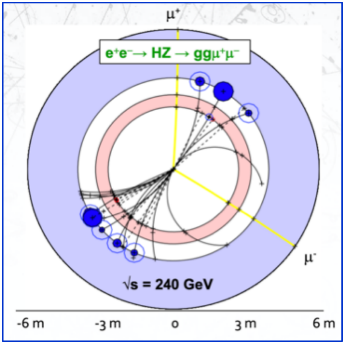

pp collision event

Higgs event in pp

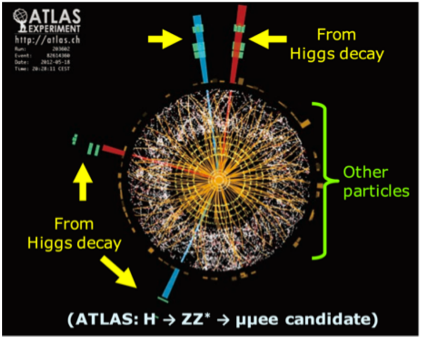

FCC-ee detector performance requirements

Higgs-strahlung

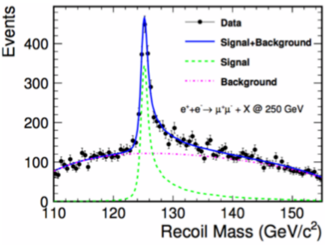

momentum resolution

WW fusion

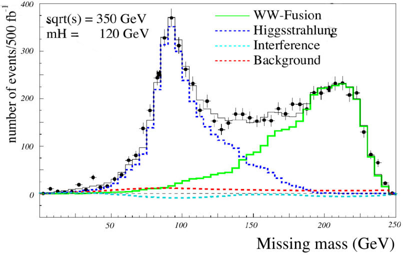

jet energy resolution

M_H = 125 GeV	SM BF
bb	56.1%
WW*	23.1%
gg	8.2%
ττ	6.3%
ZZ*	2.6%
cc	2.9%
γγ	0.2%
Zγ	0.15%
ss	0.1%
μμ	0.02%

flavour tagging

Particle ID

- $\frac{\delta p_T}{p_T} \sim 0.1\%$ for $p_T \sim 50$ GeV (to commensurate with beam energy spread).
- Jet energy resolution of $\frac{30\%}{\sqrt{E}}$ in multi-jet environment for Z/W separation.
- Superior impact parameter resolution for c and b tagging.

Charged particle trajectories in the inner detector

$$d\alpha = \frac{dp}{p} = \frac{qvBdt}{p} = \frac{q}{p}B \underbrace{vdt}_{=ds=dr} = \frac{q}{p}Bds.$$

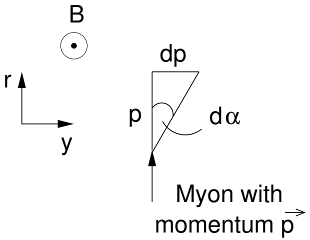

Hence we get

$$\alpha(r) \approx \frac{q}{p}\int_{r_0}^{r} B(s)ds$$

and

$$y(r) = \int_{r_0}^{r} \alpha(r')dr' = \frac{q}{p}\int_{r_0}^{r}\int_{r_0}^{r'} B(s)\,ds\,dr'.$$

Beispiel. $p = 1$ GeV. $r_0 = 0$. $B = 2$ T.
$\alpha(10$ cm$) = 60$ mrad. $y(10$ cm$) = 3$ mm.
$\alpha(1$ m$) = 0,6$ rad. $y(1$ m$) = 30$ cmm.

Momentum resolution in the inner detector

- Deflection angle at distance r from the pp interaction point:

$$\alpha(r) = \frac{q}{p} \int_0^r B\, ds$$

- Total deflection angle: $\alpha := \alpha(r_{max})$ (r_{max} radius of the inner detector).
- Error propagation:

$$\delta\alpha = \frac{|q|}{p^2} \int_0^{r_{max}} B\, ds \cdot \delta p = \alpha \cdot \frac{\delta p}{p} \Leftrightarrow \frac{\delta p}{p} = \frac{\delta\alpha}{\alpha}$$

$$\frac{\delta p}{p} = \frac{\delta\alpha}{\frac{|q|}{p} \int_0^{r_{max}} B\, ds}$$

Momentum resolution in the inner detector

$$\frac{\delta p}{p} = \frac{\delta\alpha}{\frac{|q|}{p}\int\limits_0^{r_{max}} B\,ds}$$

- Contributions to $\delta\alpha$

$$\delta\alpha = \sqrt{(\delta\alpha_{mult.\ scattering})^2 + (\delta\alpha_{detector\ resolution})^2}$$
$$= \sqrt{\left(13,6\ \text{MeV}\sqrt{\frac{D}{X_0}}\right)^2 + (\delta\alpha_D)^2}$$

Hence

$$\frac{\delta p}{p} = \frac{13,6\ \text{MeV}\sqrt{\frac{D}{X_0}}}{|q|\int B\,ds} \oplus \frac{\delta\alpha_D}{|q|\int B\,ds}\cdot p$$

⇒ Best possible momentum given by the ratio of multiple scattering and the magnetic field integral.

⇒ High momenta (small values of α): Momentum resolution determined by the ratio of the spatial resolution of the detector and the magnetic field integral. The momentum resolution degrades with increasing p.